Proc. 7th Int. Symp. Diamond Maters., Electrochem Soc PV-2001-25
(Penington, NJ, USA, 2001)

THE INFLUENCE OF SURFACE TERMINATION ON THE ELECTROCHEMICAL PROPERTIES OF BORON DOPED DIAMOND

Matthew Alexander, Matthew N. Latto, Gustavo Pastor-Moreno and D. Jason Riley
School of Chemistry, University of Bristol, Cantock's Close,
Bristol BS8 1TH, United Kingdom.

There is considerable interest in electrodes fabricated from boron doped CVD diamond. Using highly doped samples it has been demonstrated oxidative and reductive processes can occur at such electrodes. The properties of diamond have led to the suggestion that electrodes fabricated from this material may offer advantages in environments in which both chemical or mechanical robustness is of importance. This paper is concerned with electrochemical studies of low boron doped CVD diamond. The method of preparation is detailed and a novel technique of forming an Ohmic contact to the diamond described. The results of studies of simple outer sphere electron transfer reactions at the electrode are detailed and the effect of altering the surface termination described. The results obtained are discussed in relation to a surface state mediated electron transfer mechanism.

INTRODUCTION

The advent of reproducible inexpensive methods of diamond film preparation using chemical vapour deposition (CVD) technology has resulted in exploration of the wide-ranging applications of this material. A major area of advancement in the past decade has been the use of boron doped CVD diamond in electrochemistry (1-15). It has been proposed that boron doped CVD diamond films may be employed as stable electrodes in various electrochemical processes. Due to the fact that diamond is chemically inert, electrodes formed from this material offer advantages over metals, particularly for electrosynthesis in harsh environments (4,16).

Doping of diamond in the CVD process is generally achieved by introducing a gaseous boron species to the reaction chamber. It has been demonstrated that the level of boron doping in the diamond film is directly proportional to the amount of boron in the feed gas (17). The majority of electrochemical studies of boron doped CVD diamond have been concerned with samples prepared using high levels of boron, greater than 1000 ppm boron to carbon ratio, in the feed gas, we refer to such samples as being highly doped. In aqueous electrolytes containing no electroactive species potential scans at highly doped diamond electrodes indicate oxygen evolution occurs at anodic potentials and hydrogen evolution at cathodic potentials. The potential window in aqueous solution of boron doped CVD diamond is greater than that observed for other electrode materials (18). The possibility of utilising this increased potential range has been realised in the efficient reduction of nitrate to ammonia (2). Electrochemical studies of highly boron doped CVD diamond performed in aqueous electrolyte using outer sphere reversible

redox couples display current-voltage signatures characteristic of metal electrodes. This suggests that at such electrodes the applied overpotential is dropped across the Helmholtz layer, i.e. the diamond is degenerately doped. However, capacitance studies at boron doped CVD diamond show that $1/C^2$ is proportional to the applied potential, i.e. Mott-Shottky behaviour, and that the applied overpotential is dropped across the space charge region. This dichotomy has been explained by invoking electron transfer via surface states (1). Support for this hypothesis has been obtained from impedance studies of both single crystal (19) and CVD boron doped diamond (20) in which two time constant for the electron transfer process have been observed.

When considering electron transfer at a semiconductor solution interface the theoretical approach developed by Gerischer and based on the overlap between electronic states on solution based species and the electrode is instructive (21,22). The surface state mediated mechanism of charge transfer that can account for the observation of both oxidative and reductive Faradaic currents under depletion conditions is shown, for a p-type semiconductor, in figure 1. It is apparent that in the absence of any surface states the degree of hole transfer would be negligible as the density of majority charge carriers at the semiconductor surface would be small. Surface states act as charge carrier sinks at the electrode surface and hence mediate charge transfer to redox couples. Figure 1a shows the p-type semiconductor / surface state / electrolyte interface at equilibrium. An applied overpotential is partitioned between the Helmholtz layer, assuming a high concentration of background electrolyte, and the space charge layer. Figure 1b depicts the situation when a positive overpotential is applied, it is apparent that oxidation may

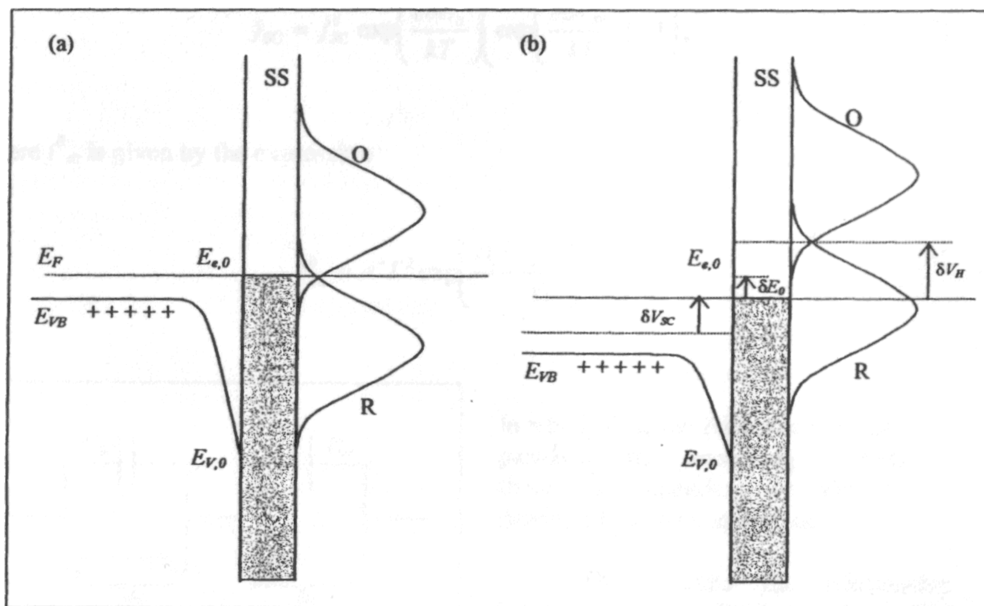

Figure 1 - The surface state (SS) mediated mechanism of electron transfer at a p-type semiconductor solution interface. (a) Shows the energy levels at equilibrium and (b) depicts the situation when a positive overpotential is applied. The vertical axis is electron energy and on the electrode side E_{VB} is the energy of the occupied (+) valance band and the shaded area represents the level to which the surface states are occupied. The Gaussian curves on the solution side of the interface depict the state density distribution for the oxidised and reduced redox species.

occur via a two step process; electron transfer from the reduced species to the surface state and then hole transfer from the bulk semiconductor to the surface state. The current flowing will be dependent upon the relative rates of electron transfer across the two interfaces. The equilibrium between the redox couple and surface states is akin to a metal-redox couple whilst the surface state / semiconductor junction can be modelled as a Schottky barrier. If electron transfer across the space charge region is rate limiting then the electrode will behave like a semiconductor whilst when electron transfer across the Helmholtz layer is rate limiting then the electrode will resemble a metal. As discussed above the majority of boron doped CVD diamond samples studied have been highly doped and when a redox couple is present in solution they show electrochemical behaviour characteristic of a metal, suggesting electron transfer across the Helmholtz layer is rate limiting.

To investigate further the electron transfer process at the CVD diamond electrode / electrolyte interface we have undertaken electrochemical studies of low boron doped CVD diamond. This paper is concerned with the preparation and characterisation of CVD diamond samples in which the boron level in the feed gas was less than 50 ppm. The electrochemical behaviour of the as prepared diamond was investigated and the effect of changing the surface termination on the electron transfer process considered. The low doping level employed and the requirement that chemical treatment of the surface should be facile necessitated the preparation of a high quality, buried Ohmic contact. A novel method of preparing such a contact is described. The results obtained are discussed in terms of surface state mediated electron transfer.

THEORY

Two approaches have been taken to explain the relationship between potential and current for those systems that undergo surface state mediated charge transfer processes. Both models consider the interface as consisting of two elements in series; the space charge layer and the Helmholtz layer. Chazalviel (23) considers the situation at an n-type semiconductor and assumes that current flowing across the space charge region can be calculated using Schottky diode theory whilst the charge across the Helmholtz layer can be derived from Marcus theory. To facilitate the calculation of the current density as a function of potential Chazalviel only considers interfaces for which the Helmholtz layer capacitance is very much greater than the space charge layer capacitance, i.e., interfaces with a low density of surface states. In a more detailed analysis Vanmaekelbergh (24,25) discusses the potential dependence of all four steps in the surface mediated charge transfer process; forward and reverse electron transfer between the bulk semiconductor and the surface state and forward and reverse electron transfer between the surface state and the solution phase redox species. Vanmaekelbergh has employed the theory to explain the current versus potential curves obtained at a boron doped single crystal diamond electrode. Below we develop the Chazalviel approach to account for p-type semiconductors with a high density of surface states, i.e., electrodes for which the potential drop across the Helmholtz layer changes with applied potential.

Figure 1a depicts the electrode-electrolyte interface at equilibrium. The Fermi level for the bulk semiconductor, the surface states and the solution phase redox couple lies at a common energy, $E_{e,0}$. The situation when a positive overpotential of magnitude δV is applied is shown in figure 1b. The applied bias is dropped across the space charge layer, δV_{SC}, and the Helmholtz layer, δV_H. The applied bias results in a change in the energy distribution of electrons in the surface state and a change in the Fermi energy of these electrons, expressed in eV as δE_0. Assuming that (i) Marcus theory (26) for electron transfer between the surface states and the redox couple is valid and (ii) the transfer coefficient is 0.5, the expression for the current density across the Helmholtz layer, j_H, is

$$j_H = 2j_H^0\left(\sinh\left(\frac{e\delta V_H}{2kT}\right)\right), \qquad [1]$$

where e is the modulus of the charge on an electron, k is Boltzmann's constant and T is the temperature. If it is assumed that the boundary between the bulk semiconductor and the surface states can be modelled as a Schottky barrier (27) then the current across this junction, j_{SC}, is

$$j_{SC} = j_{SC}^0 \exp\left(\frac{e\delta E_0}{kT}\right)\left(\exp\left(\frac{e\delta V_{SC}}{kT}\right)-1\right), \qquad [2]$$

where j^0_{sc} is given by the expression

$$j_{SC}^0 = A^* T^2 \exp\left(\frac{e\left(E_{V,0} - E_{e,0}\right)}{kT}\right), \qquad [3]$$

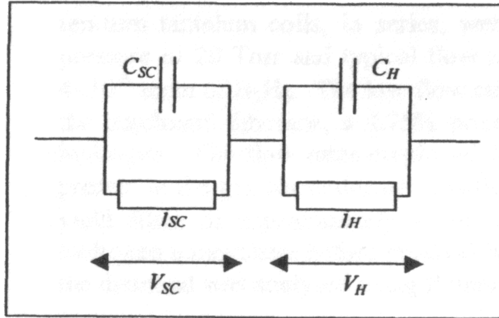

Figure 2 - Equivalent circuit for the interface. V_{SC} represents the potential drop across the space charge region and V_H that across the Helmholtz layer.

in which A^* is the Richardson constant, a parameter that according to diffusion theory is dependent on the doping density of the semiconductor.

To calculate the relationship between current density and applied overpotential it is necessary to consider how the applied potential is related to δV_{SC} and δV_H. Figure 2 shows the equivalent circuit for the interface. Applying Kirchoff's laws gives

$$j_{SC} + C_{SC}\frac{\mathrm{d}V_{SC}}{\mathrm{d}t} = j_H + C_H\frac{\mathrm{d}V_H}{\mathrm{d}t}, \qquad [4]$$

which given that $V = V_H + V_{SC}$ may be written as

$$\frac{\mathrm{d}V_H}{\mathrm{d}t} = (1-\gamma)\frac{\mathrm{d}V}{\mathrm{d}t} + \left(\frac{1}{C_H + C_{SC}}\right)\frac{\mathrm{d}Q_{ss}}{\mathrm{d}t}, \qquad [5]$$

where γ is $C_H / (C_H + C_{SC})$ and Q_{ss} is the charge on the surface states. If the density of surface states per eV is $\rho(E_0)$ then $\mathrm{d}Q_{ss} = e\rho(E_0)\mathrm{d}E_0$. Hence is if C_H, C_{sc} and $\rho(E_0)$ are potential independent the expressions for δV_H and δV_{SC} are

$$\delta V_H = (1-\gamma)\delta V + \beta\delta E_0 \qquad [6]$$

$$\delta V_{SC} = \gamma\delta V - \beta\delta E_0 . \qquad [7]$$

Eliminating δE_0, δV_{SC} and δV_H from equations [1] and [2] yields

$$j_{SC} = j_{SC}^0 \exp\left(-\frac{e}{\beta kT}\left[(1-\gamma)\delta V - \frac{2kT}{e}\sinh^{-1}\left(\frac{j_H}{2j_H^0}\right)\right]\right) \times \left(\exp\left(\frac{e}{kT}\left[\delta V - \frac{2kT}{e}\sinh^{-1}\left(\frac{j_H}{2j_H^0}\right)\right]\right) - 1\right) \qquad [8]$$

Whan for a particular potential a steady-state current is achieved $j_{SC} = j_H = j$, hence equation [8] may be written as

$$j = j_{SC}^0 \exp\left(-\frac{e}{\beta kT}\left[(1-\gamma)\delta V - \frac{2kT}{e}\sinh^{-1}\left(\frac{j}{2j_H^0}\right)\right]\right) \times \left(\exp\left(\frac{e}{kT}\left[\delta V - \frac{2kT}{e}\sinh^{-1}\left(\frac{j}{2j_H^0}\right)\right]\right) - 1\right) \qquad [9]$$

Using suitable algorithms it is possible, for a particular overpotential, to find values of j that satisfy the above equality.

Simulations of current versus voltage curves for three different sets of parameters are shown in figure 3. It is apparent that the behaviour of the electrode can vary between that of a metal and that of an ideal p-type semiconductor. A response characteristic of a metallic electrode is obtained when $j^0_H >> j^0_{SC}$ whilst semiconductor behaviour is observed when $j^0_H << j^0_{SC}$. At intermediate values a complex response is observed in which both a oxidative and reductive current is observed but the oxidation process is less resistive than the reduction.

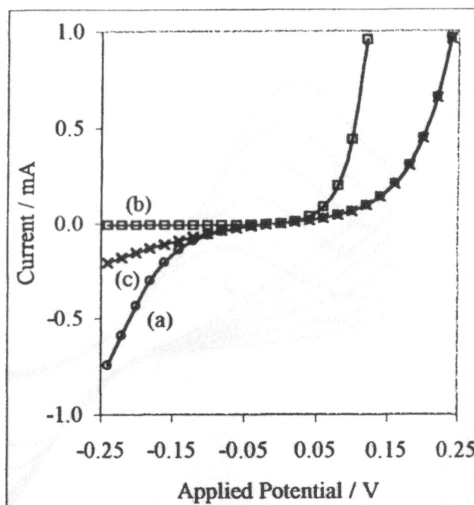

Figure 3 - Current versus voltage curves for surface state mediated charge transfer.
(a) $\beta = 1, \gamma = 1, j^0_H = 10^{-6}$ A, $j^0_{sc} = 10$ A.
(b) $\beta = 1, \gamma = 1, j^0_H = 10$ A, $j^0_{sc} = 10^{-6}$ A.
(c) $\beta = 1, \gamma = 1, j^0_H = 10^{-5}$ A, $j^0_{sc} = 10^{-3}$ A.

EXPERIMENTAL

Undoped silicon (100) wafers of approximately 1cm by 2 cm in dimension were employed as substrates for diamond growth. In preparing the substrate a 3 mm strip of the silicon was masked and then the exposed area was manually abraded with 1-3 μm diamond grit. After removal of the mask the silicon was ultrasonically cleaned in propan-2-ol. A 5 mm strip of titanium of thickness 100 nm was then evaporated on to the silicon, straddling the unabraded and abraded regions. Boron doped CVD diamond was then deposited on to the substrate.

A hot filament reactor was used to deposit the diamond. Two 0.25 mm diameter, ten-turn tantalum coils, in series, were used as filaments. The film was grown at a pressure of 20 Torr and typical flow rates were 200 sccm of H_2, 1.4 sccm of CH_4 and 4×10^{-5} sccm of B_2H_6. The low flow rate of the diborane was achieved by pre-dilution of the purchased diborane, a 4.75% premix of diborane in hydrogen from BOC, in more hydrogen. The flow rates employed indicate a boron to carbon ration of 50 ppm was present in the gas phase during growth. Deposition runs of 12 hours were employed to yield films of approximately 4 μm thickness. The film was allowed to cool in a hydrogen atmosphere before removal from the chamber. Prior to electrochemical studies the diamond was analysed using Raman spectroscopy.

Inspection of the as prepared surface using an optical microscope indicated that a continuous diamond film had grown on both the silicon and abraded titanium substrate

but on the unabraded titanium surface, on which there was no nucleation sites, no diamond was visible. Electrical contact to the low doped diamond film was therefore easily achieved by bonding a copper wire to the uncoated titanium surface. Electrochemical experiments were performed on as-prepared boron doped CVD diamond samples, referred to as hydrogen terminated and on diamond electrodes that had been treated with chromic acid in order to achieve oxygen termination.

Cyclic voltammetric studies of the low doped diamond samples were carried out in nitrogen purged aqueous solutions that were equimolar in $Fe[CN]_6^{3-}$ and $Fe[CN]_6^{4-}$ and contained 0.1 mol dm^{-3} of potassium chloride. A three electrode system was used; a diamond working electrode, a platinum gauze counter electrode and a silver / silver chloride reference electrode. All potentials are reported relative to the silver / silver chloride reference electrode. The diamond electrode was mounted in the cell such that 0.3 cm^2 of the diamond surface was exposed to electrolyte. The cyclic voltammograms were recorded using an ecochemie μautolab potentiostat and associated software.

RESULTS

A Raman spectrum of the as prepared diamond, obtained using a laser of wavelength 514.5 nm, is shown in figure 4. A sharp Raman peak at 1332 cm^{-1} corresponding to sp^3 hybridised carbon was observed and no sp^2 peak was apparent, indicating that the diamond electrodes were of high quality. To ensure that the electrical contacts to the low doped diamond samples were Ohmic a sample with two titanium strips was prepared and the current flowing between the two regions as a function of applied potential monitored. The current-voltage response obtained is displayed in figure 5. It is apparent that the novel method of preparing electrical connection to low doped diamond samples yields contacts that are Ohmic.

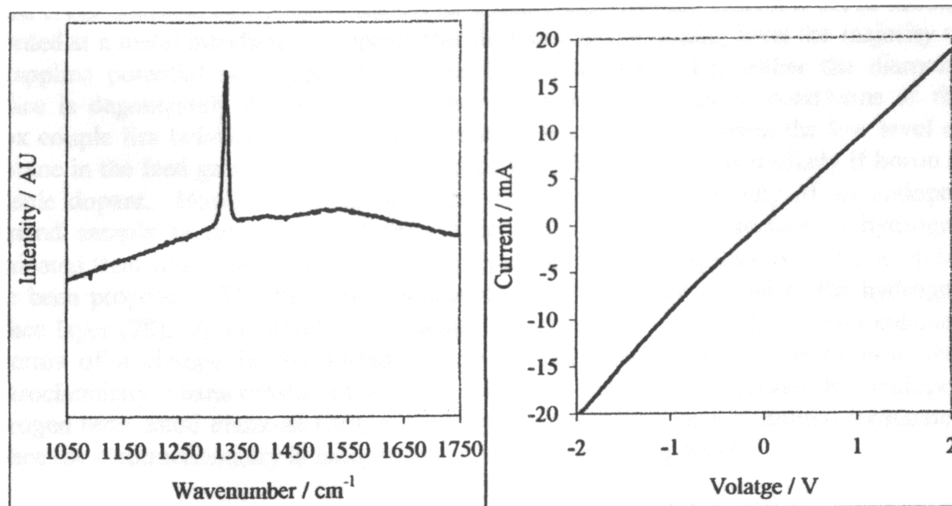

Figure 4 - A Raman spectrum of the as prepared low boron doped CVD diamond electrode. The spectrum was recorded using an excitation wavelength of 514.5 nm.

Figure 5 - The current flowing as a function the applied volatge between two buried titanium contacts.

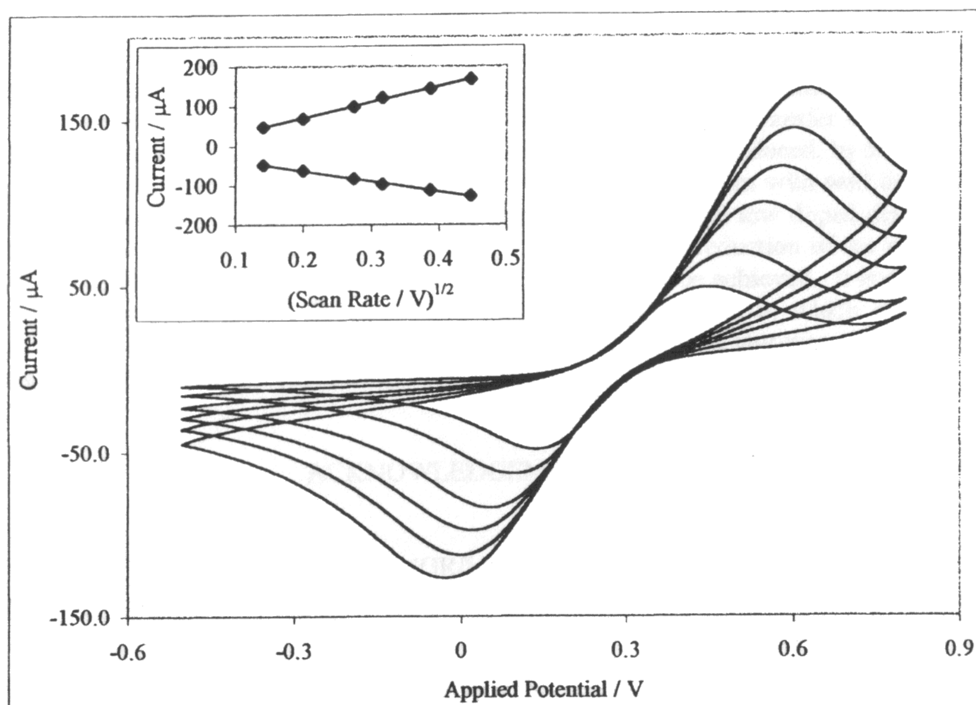

Figure 6 - Cyclic voltammogram of hydrogen terminated low boron doped CVD diamond immersed in a 0.01 mol dm^{-3} $Fe[CN]_6^{3-}$, 0.01 mol dm^{-3} $Fe[CN]_6^{4-}$ and 0.1 mol dm^{-3} KCl aqueous solution. Cyclic voltammograms for scan rates of 20 mV s^{-1}, 40 mV s^{-1}, 75 mV s^{-1}, 100 mV s^{-1}, 150 mV s^{-1} and 200 mV s^{-1} are displayed. The inset shows the anodic and cathodic currents as a function of the square root of the scan rate.

Cyclic voltammograms, recorded at a series of scan rates, for a low doped hydrogen terminated CVD diamond working electrode immersed in a 0.1 mol dm^{-3} solution of potassium chloride containing 0.01 mol dm^{-3} of both ferricyanide and ferrocyanide ions is displayed in figure 6. Both oxidation and reduction peaks are observed and a plot of peak height versus the square root of the scan rate is linear, see inset of figure 6. At all scan rates the peak height of the forward peak is identical to the peak height of the reverse peak indicating that the redox process is reversible. The peak separation is greater than 59 mV and varies with scan rate as no correction was made for the Ohmic drop across the system.

The curve in figure 7a is a cyclic voltammogram, recorded at a scan rate of 0.200 V s^{-1} for a low doped oxygen terminated CVD diamond sample immersed in the same solution. It is of note that the reduction peak is highly distorted. Figure 7b shows a cyclic voltammogram of the same oxygen terminated electrode immersed in a solution containing only 1.5 mmol dm^{-3} of both ferricyanide and ferrocyanide ions. It is apparent that for the more dilute solution a reduction peak is observed.

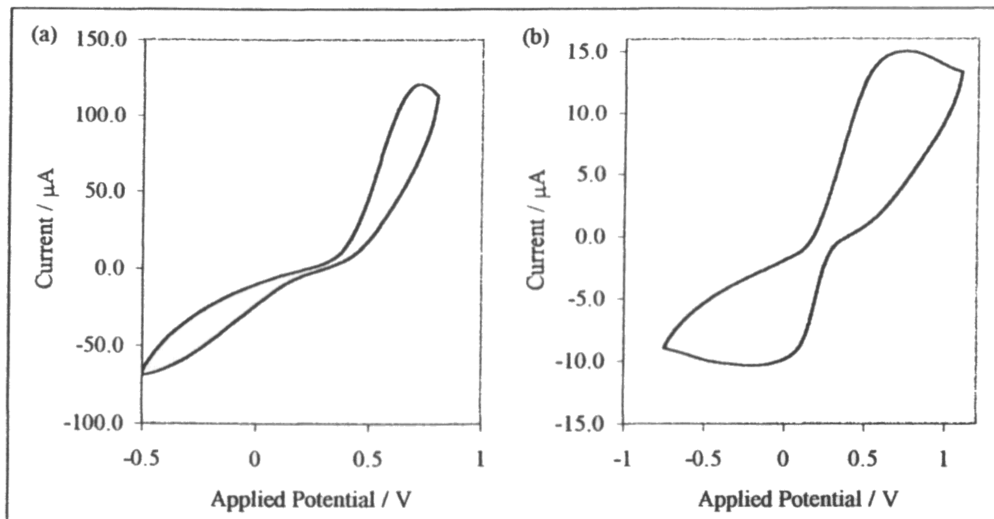

Figure 7 - Cyclic voltammograms of oxygen terminated low boron doped CVD diamond immersed in aqueous solutions equimolar in $Fe[CN]_6^{3-}$ and $Fe[CN]_6^{4-}$ and containing 0.1 mol dm^{-3} KCl aqueous solution. Cyclic voltammogram (a) shows the response when 10 mmol dm^{-3} of the redox couple was present and a scan rate of 200 mV s^{-1} was employed. (b) displays the result, recorded at a scan rate of 100 mV s^{-1}, for a solution containing 1.5 mmol dm^{-3} of the redox couple.

DISCUSSION AND CONCLUSION

The results obtained indicate that the electrochemical behaviour of a diamond electrode is dependent upon the surface termination. The hydrogen terminated low boron doped CVD diamond electrode yields cyclic voltammograms that resemble those usually recorded at a metal interface. It appears that despite the low doping level the majority of the applied potential is dropped across the Helmholtz layer, i.e., either the diamond surface is degenerately doped or the surface is under accumulation conditions as the redox couple lies below the valence band edge of the diamond. Given the low level of diborane in the feed gases degenerate doping of the CVD diamond is unlikely if boron is the sole dopant. However, it has been reported that the conductivity of an undoped diamond sample is two orders of magnitude greater when the surface is hydrogen terminated than when the surface is oxygen terminated. Two explanations of this effect have been proposed. The first invokes acceptor levels that are related to the hydrogen surface layer (28). Alternatively, the change in surface conductivity has been explained in terms of a change in the surface energy of the bands (29). It is of note that electrochemistry characteristic of a metal electrode has been observed for undoped hydrogen terminated diamond (30), a result that suggest that for a hydrogen terminated surface the electrochemistry is independent of the boron doping level.

The cyclic volatmmogram of the oxygen terminated low boron doped CVD diamond electrode immersed in the solution containing a high concentration of the redox couple shows an oxidation peak but only limited cathodic current. Comparison with the theoretical data displayed in figure 3c, in which diffusion is not taken into account,

suggests that the electron transfer process occurs via a surface mediated mechanism in which the applied potential is distributed between the space charge layer and the Helmholtz layer. Consideration of the theory indicates that electrochemical behaviour characteristic of a metal should be obtained if the rate of electron transfer across the Helmholtz layer is reduced. Figure 7b indicates that when the j^0_H is reduced, by lowering the concentration of the electroactive species, a cyclic voltammogram with well defined cathodic and anodic currents is obtained. To obtain behaviour at a low doped diamond electrode that is characteristic of a semiconductor either further reduction of the doping density is required or a change in the surface state density must be achieved. It is of note that using low boron doped diamond in non-aqueous electrolytes, in which electron transfer processes at energies where the density of surface states is low may be studied, rectifying electrochemical behaviour has been observed [ours].

ACKNOWLEDGEMENTS

The financial support of the EPSRC (GR/L84308) and the University of Bristol are gratefully acknowledged.

REFERENCES

1. S. Alehashem, F. Chambers, J. W. Strojek, G. M. Swain, and R. Ramesham, *Anal. Chem.*, **67**, 2812 (1995).

2. F. Bouamrane, A. Tadjeddine, J. E. Butler, R. Tenne, and C. Levy-Clement, *J. Electroanal. Chem.*, **405**, 95 (1996).

3. F. Bouamrane, A. Tadjeddine, R. Tenne, J. E. Butler, R. Kalish, and C. Levy-Clement, *J. Phys. Chem. B*, **102**, 134 (1998).

4. R. G. Compton, F. Marken, C. H. Goeting, R. A. J. McKeown, J. S. Foord, G. Scarsbrook, R. S. Sussman, and A. J. Whitehead, *Chem.Commun.*, 1961 (1998).

5. C. H. Goeting, F. Jones, J. S. Foord, J. C. Eklund, F. Marken, R. G. Compton, P. R. Chalker, and C. Johnston, *J. Electroanal. Chem.*, **442**, 207 (1998).

6. T. Kuo, R. L. McCreery, and G. M. Swain, *Electrochemical and Solid-State Letters*, **2**, 288 (1999).

7. L.-F. Li, S. Totir, B. Miller, G. Chottiner, A. Argoitia, J. C. Angus, and D. Scherson, *J. Am. Chem. Soc.*, **119**, 7875 (1997).

8. A. Manivannan, D. A. Tryk, Fujishima, and A., *Electrochemical and Solid-State Letters*, **2**, 455 (1999).

9. S. Nakabayashi, D. A. Tryk, A. Fujishima, and N. Ohta, *Chem. Phys. Lett.*, **300**, 409 (1999).

10. S. Nakabayashi, N. Ohta, and A. Fujishima, *PCCP*, **1**, 3993 (1999).

11. Y. V. Pleskov, A. Y. Sakharova, E. V. Kasatkin, and V. A. Shepelin, *J. Electroanal. Chem.*, **344**, 401 (1993).

12. Y. V. Pleskov, Y. E. Evstefeeva, M. D. Krotova, and A. V. Laptev, *Electrochimica Acta*, **44**, 3361 (1999).

13. G. M. Swain and R. Ramesham, *Anal. Chem.*, **65**, 345 (1993).

14. G. Swain, *Advanced Materials*, **6**, 388 (1994).

15. T. Yano, E. Popa, D. A. Tryk, K. Hashimoto, and A. Fujishima, *J. Electrochem. Soc.*, **146**, 1081 (1999).

16. C. H. Geoting, J. S. Foord, F. Marken, and R. G. Compton, *Diamond and Related Materials*, **9**, 824 (1999).

17. M. Werner, R. Job, A. Zaitzev, W. R. Fahrner, W. Seifert, C. Johnston, and P. R. Chalker, *Phys. Stat. Sol. A*, **154**, 385 (1996).

18. H. B. Martin, A. Argoitia, J. C. Angus, A. B. Anderson, and U. Landau, *Applications of Diamond Films and Related Materials: Third International Conference*, 91 (1995).

19. J. van de Lagemaat, D. Vanmaekelbergh, and J. J. Kelly, *J. Electranal. Chem.*, **475**, 139 (1999).

20. M. N. Latto, D. J. Riley, and P. W. May, *Diamond and Related Materials*, **9**, 1181 (2000).

21. H. Gerischer, *Z. Phys. Chem. N.F.*, **27**, 48 (1961).

22. H. Gerischer, *J. Phys. Chem.*, **95**, 1356 (1991).

23. J.-N. Chazalviel, *J. Electrochem. Soc.*, **129**, 963 (1982).

24. D. Vanmaekelbergh, *Electrochimica Acta*, **42**, 1121 (1997).

25. D. Vanmaekelbergh, *Electrochimica Acta*, **42**, 1135 (1997).

26. R. A. Marcus, *J. Chem. Phys.*, **43**, 679 (1965).

27. S. M. Sze, *Physics of Semiconductor Devices,* 2nd edition, p. 258, Wiley Interscience, New York (1981).

28. H. Kiyota and E. Matsushima, *Appl. Phys. Lett.*, **67**, 3596 (1995).

29. J. Ristein, *Diamond and Related Materials*, **9**, 1129 (2000).

30. R. Ramesham, *Thin Solid Films*, **315**, 222 (1998).

31. G. Pastor-Moreno and D.J. Riley, *Electrochimica Acta*, submitted.